AD

TECHNICAL REPORT ARCCB-TR-95036

INDUCED OVERLOAD RESIDUAL STRESSES IN EX35 MULTI-LUG BREECH RING

S.L. LEE
M.J. GLENNON
A. GABRIELE

AUGUST 1995

US ARMY ARMAMENT RESEARCH,
DEVELOPMENT AND ENGINEERING CENTER
CLOSE COMBAT ARMAMENTS CENTER
BENÉT LABORATORIES
WATERVLIET, N.Y. 12189-4050

DISCLAIMER

The findings in this report are not to be construed as an official Department of the Army position unless so designated by other authorized documents.

The use of trade name(s) and/or manufacturer(s) does not constitute an official indorsement or approval.

DESTRUCTION NOTICE

For classified documents, follow the procedures in DoD 5200.22-M, Industrial Security Manual, Section II-19 or DoD 5200.1-R, Information Security Program Regulation, Chapter IX.

For unclassified, limited documents, destroy by any method that will prevent disclosure of contents or reconstruction of the document.

For unclassified, unlimited documents, destroy when the report is no longer needed. Do not return it to the originator.

REPORT DOCUMENTATION PAGE

Form Approved
OMB No. 0704-0188

1. AGENCY USE ONLY (Leave blank)	2. REPORT DATE	3. REPORT TYPE AND DATES COVERED
	August 1995	Final

4. TITLE AND SUBTITLE
INDUCED OVERLOAD RESIDUAL STRESSES IN EX35 MULTI-LUG BREECH RING

5. FUNDING NUMBERS
AMCMS: 6111.02.H611.1

6. AUTHOR(S)
S.L. Lee, M.J. Glennon, A. Gabriele

7. PERFORMING ORGANIZATION NAME(S) AND ADDRESS(ES)
U.S. Army ARDEC
Benét Laboratories, AMSTA-AR-CCB-O
Watervliet, NY 12189-4050

8. PERFORMING ORGANIZATION REPORT NUMBER
ARCCB-TR-95036

9. SPONSORING / MONITORING AGENCY NAME(S) AND ADDRESS(ES)
U.S. Army ARDEC
Close Combat Armaments Center
Picatinny Arsenal, NJ 07806-5000

10. SPONSORING / MONITORING AGENCY REPORT NUMBER

11. SUPPLEMENTARY NOTES
Presented at the ASME Pressure Vessel & Piping Conference, Honolulu, Hawaii, 23-27 July 1995. Published in the Conference Proceedings.

12a. DISTRIBUTION / AVAILABILITY STATEMENT
Approved for public release; distribution unlimited

12b. DISTRIBUTION CODE

13. ABSTRACT (Maximum 200 words)

An exploratory prototype multi-lug breech block/ring assembly was designed for future projectile launchers. The new geometry redistributes the applied load to several surfaces rather than one surface in conventional breech to react the load. Induced residual stresses from shot peening and overload processes improve fatigue life of the system. In this work, experimental x-ray diffraction residual stress mapping was performed in the lugs of the unaffected portion of a 50 percent overloaded multi-lug breech ring that was fatigue tested to failure. Finite element modelling of a two-dimensional cross section of the breech block/ring assembly was performed using ABAQUS codes on a Convex C-220 computer. Comparisons of experimental residual stresses and finite element analysis (FEA) predictions showed good agreement in the major features of residual stress distribution, especially in the front lug. While FEA predicted the general characteristics of experimental residual stress distribution, experimental residual stresses were deeper and less compressive.

14. SUBJECT TERMS
Multi-Lug Breech, Breech Mechanism, Overload Process, EX35, Residual Stress, Finite Element Analysis

15. NUMBER OF PAGES
21

16. PRICE CODE

17. SECURITY CLASSIFICATION OF REPORT	18. SECURITY CLASSIFICATION OF THIS PAGE	19. SECURITY CLASSIFICATION OF ABSTRACT	20. LIMITATION OF ABSTRACT
UNCLASSIFIED	UNCLASSIFIED	UNCLASSIFIED	UL

TABLE OF CONTENTS

ACKNOWLEDGEMENTS iii

INTRODUCTION 1

MULTI-LUG BREECH MECHANISM 1

OVERLOAD MANUFACTURE PROCESS 2

X-RAY EXPERIMENTAL METHODS 2

HOOP AND RADIAL DIRECTIONS IN THE LUGS 3

RESIDUAL STRESSES IN THE FAILED ARM 3

FRONT LUG HOOP RESIDUAL STRESSES 3

MIDDLE LUG HOOP RESIDUAL STRESSES 4

RADIAL RESIDUAL STRESS DISTRIBUTION 4

FINITE ELEMENT MODELLING 4

COMPARISON OF EXPERIMENTAL RESULTS AND FEA PREDICTIONS 5

CONCLUSION 6

REFERENCES 7

List of Illustrations

1. Multi-Lug Breech Block/Ring Assembly 8

2. Comparison of Multi-Lug Breech System and Conventional Breech System 9

3. Cross-Sectional and Vertical Residual Stress Analysis in Multi-Lug Breech Ring 10

4. Geometry of Front and Middle Lugs and Directions of X-ray Stress Analysis 11

5. Hoop Residual Stresses in the Front Lug 12

6. Hoop Residual Stresses in the Middle Lug 13

7. Radial Versus Hoop Residual Stresses in the Front Lug 14

8. ABAQUS Finite Element Mesh of the Breech Ring/Block Assembly 15

9. ABAQUS Von Mises and Principal Stresses 16

10. Experimental and ABAQUS Surface Hoop Stress Comparison in the Front Lug 17

11. Experimental and ABAQUS Hoop Stress Distribution Comparison in the Front Lug 18

ACKNOWLEDGEMENTS

Thanks to Dr. Peter Chen and Mr. John Underwood of Benét Laboratories for their critical review of the manuscript. Thanks also to Ellen Fogarty for her editorial review of the manuscript.

INTRODUCTION

To improve the conventional slide block breech mechanism in future projectile launchers, exploratory multi-lug breech systems consisting of a series of modified lugs have been designed. Figure 1 shows the multi-lug breech block/ring assembly where the connection to the pressure chamber is to the right of the assembly. Geometry in the new and lighter breech diffuses the concentrated stresses found at the block/ring interface of conventional breeches (ref 1). Development commenced with finite element analyses (FEA) of an optimized configuration by varying the number of lugs, contact interface angles, fillet radii, flank angles, relative lug sizes, and distance between the lugs.

An inside diameter shot peening technique and overload process using an overload fixture generated advantageous residual stress distribution in the lugs (refs 2,3). The compressive surface residual stress induced in the lugs greatly increases the fatigue life of the breech. Shot peened and overload-induced residual stresses were comparable in magnitude, but the residual stresses produced in the overload process were much deeper than in the shot peening process. X-ray diffraction measurements of residual strains were also compared to strain gage measurements along the circumference of the lugs. Based on the x-ray data, the overload process was preferred over the shot peening process for inducing residual stresses in the multi-lug breech (ref 3). In a shot peened, swaged, and tensile overload notched-bend specimen, the highest life was measured from overload specimens that had the deepest and highest surface residual stress distribution (ref 4).

In this work, a prototype multi-lug breech block/ring assembly made of 4340 steel was overloaded to 150 percent of chamber design pressure by an overload fixture. Residual stress distribution was determined by a position-sensitive multiple-exposure x-ray diffraction technique. Minimum data were obtained in the failed arm of the multi-lug breech where redistribution of residual stresses was observed. Residual stress mapping in the front and middle lugs of the unaffected portion of the opposite arm was made. Finite element modelling of a two-dimensional cross section of the breech block/ring assembly was performed using ABAQUS codes on a Convex C-220. A comparison of experimental residual stresses and FEA predictions was made. While FEA predicted the general characteristics of experimental residual stress distribution, experimental residual stresses were deeper and less compressive.

MULTI-LUG BREECH MECHANISM

An analytical cross section of the multi-lug breech design is compared with a conventional slide block breech in Figure 2. The breech mass is balanced about the bore center to minimize the transverse motion of the tube during projectile launch. The multi-lug configuration has three block/ring contact interfaces on each side. The number, depth, and geometry of the lugs, the block/ring contact area, contact interface angle, and the distance between lugs are designed to diffuse stress concentrations and obtain maximum stress efficient configuration. In the overload process, uniform pressure was applied to the breech block and transmitted to the breech ring through the contact region. The reversed angle of the rear lug is for the lateral control of the breech jaw. This allows the breech block to limit the lateral deflection of the ring jaws, hence the term "self-tying." Lug fillet stresses are equalized as much as possible by providing a "gap"

area at the contact surfaces.

OVERLOAD MANUFACTURE PROCESS

An overload process was performed by the application of both uniform hydraulic and mechanical pressures using an overload fixture designed by the Experimental Mechanics Branch. Overload levels of 0, 25, 50, 75, and 100 percent were investigated analytically which showed a significant gap enlargement above 75 percent overload. Therefore, limits were placed on the amount of overload pressure to avoid large changes in the gap from interfering in the breech operation. For the present work on EX35 breeches, the fatigue design chamber pressure used was 83 Ksi and 50 percent overload was applied. Specimen #23, a 50 percent overloaded downslider, was chosen for residual stress studies. Crack initiation in the breech ring was observed at 16,800 cycles and failure occurred in one of the arms of the breech ring at 26,572 cycles. Multi-lug breech failure generally occurred at the lower back of the front lug in a direction approximately 30 to 35 degrees from normal, assuming a semi-circular geometry in the front lug.

X-RAY EXPERIMENTAL METHODS

Slices one to two inches thick were cut off from both the failed arm and the unaffected portion of the good arm. An electropolishing technique was used to remove surface layers of the cross section to remove residual stresses due to machining. The polishing solution was a mixture of H_2SO_4 and H_3PO_4 acids. A total of 10 mils was removed from the surface before x-ray investigation. An omega tilt x-ray stress analyzer with a position-sensitive proportional counter decision system was used for data acquisition. Chromium radiation reflection from 211 planes of martensite steel at 156 degree two theta was used for this analysis. The elastic constant for the 211 planes of 4340 steel was determined from a four-point-bend experiment (ref 5). Error analysis includes both counting statistics errors in the proportional counter and goodness of fit of linear sin-square-psi plot. Depending on the collimator used and the count rate, x-ray stress analysis accuracies were around 5 to 10 Ksi. Errors may be larger for difficult curved surfaces or cavities.

X-ray stress analysis can be performed by irradiation on the cross section or on the surfaces inside the lugs. Residual stress measurements for most shot peened and some overloaded breeches were made in the vertical geometry by successive x-ray measurement, surface layer removal, and correction for relaxation due to layer removal. Residual stress analysis of most overloaded breeches and some shot peened breeches was performed on the cross section by using a narrow moving collimator 1 mm wide. As shown in Figure 3, cross-sectional stress measurements were made in a direction parallel to "hoop" where hoop is defined as the direction tangent to the surface at the area being considered. Distribution analysis was made along AA, AB, AC, etc. directions in the front lug, and BA, BB, BC, etc. directions in the middle lug, where AC and BC are normal to the bottom of the front and middle lugs. The tip of AA in the front lug is where failure initiated. X-ray collimator width has been taken into account in the location of depth from surface.

HOOP AND RADIAL DIRECTIONS IN THE LUGS

In studies of plastic deformation in swaged cylinders, cylindrical symmetric geometry exists and hoop and radial directions are well defined. Experimental residual stress analysis was in fair agreement with FEA calculations, with FEA predicting greater compressive stresses near the bore (ref 6). In the multi-lug breech system, symmetric geometry no longer exists. However, stress concentrations are expected in the semi-circular lugs. Because of the semi-circular geometry, experimental x-ray stress analysis and comparison with FEA results were emphasized in the hoop and radial stress distribution within the lugs, where "hoop" is defined in the previous section and "radial" is in a direction perpendicular to hoop.

Figure 4 shows the geometry of the front and middle lugs. Directions of x-ray measurements are shown superimposed on the FEA mesh. The top figure is the semi-circular front lug and directions of measurements AA, AB, AC, AD, AE, etc. The bottom figure shows the semi-circular middle lug along with measurement directions BA, BB, BC, etc. Negative angles indicate the front part of the lugs, positive angles indicate the back part of the lugs, and AC and BC are normal to the bottom of the front and middle lugs, respectively. The circular geometry is replaced by tangential geometry at the upper back of the front and middle lugs.

RESIDUAL STRESSES IN THE FAILED ARM

In the fatigue failed sample #23, the front lug of one of the arms failed. Measurements at sites near the failure site showed vanishing residual stresses in all directions as expected. Furthermore, we found that failure in the front lug caused drastic redistribution of residual stresses near the vicinity of the middle lug. Measurements made inside the lug by successive layer removal techniques were in agreement with cross-sectional measurements, taking into account high stress gradients caused by failure at certain locations. Surface residual stresses along BD and BE directions were less compressive near the surface, and subsurface residual stresses became tensile within 0.1 mm beneath the surface. In the BB and BC directions, surface stress was more compressive and remained compressive until 0.5 mm before turning tensile at 1.3 mm. Residual stress analysis in cracked or failed components can be used to study crack initiation, crack growth, and failure mechanics. In this work, x-ray analysis concentrates in the unaffected portion of the good arm opposite to the failed arm.

FRONT LUG HOOP RESIDUAL STRESSES

In the good arm, hoop residual stresses in the major directions AA, AB, AC, and AE in the front lug are given in Figure 5. The depth in each direction is given by the distance from the surface of the lug along a line perpendicular to the surface. Surface residual stress is an average of two measurements--one in the surface contour analysis and the other in the depth stress distribution analysis. Compressive residual stresses were the greatest at -110 Ksi near the bottom of the lug along AC and AB directions. AC is normal and AB is 15 degrees towards the back of the lug, considering the load is applied from the front. Hoop stress levels fall off when moving up along the sides of the lug. At the tip of site AA where the failure occurred, the maximum residual stress level was -55.3 Ksi. Crack initiation began at the tip of AA, which is

approximately 25 to 30 degrees from normal. It may be possible to further improve the performance by changing the design of the lug geometry and the location of the block/ring interface contact point in the front lug.

Hoop residual stresses fall off with depth and become tensile at greater depth. This is necessary in order to form a balanced force field in the breech. A quantity "half stress depth" is introduced, which represents the depth where residual stress falls to 50 percent of the range between maximum compressive to maximum tensile stresses. Thickness of residual stress distribution is maximum at the bottom of the lug and decreases moving up the edge of the lug. In the AC direction, half stress depth is 7 mm. In the AB direction, half stress depth is 4 mm.

MIDDLE LUG HOOP RESIDUAL STRESSES

In the good arm, hoop residual stress data along BA, BB, BC, BD, BE, and BF in the middle lug have been measured. Figure 6 gives stresses along major directions BA, BB, BC. Residual stress distribution has behavior similar to the front lug, with slightly reduced compressive stresses and thinner compressive stress layers. Experimental results show that the compressive stress level was greatest near the bottom of the lug, and that it levels off when moving up the side of the lug. The thickness of residual stress distribution is maximum at the bottom of the lug BC, and it decreases when moving up the edge of the lug. Residual stress peaked at -92 Ksi at the root of the BC direction, and the half stress depth was 4.0 mm. In the BB direction, the maximum surface compressive stress was -83 Ksi, and the half depth was 2.5 mm.

RADIAL RESIDUAL STRESS DISTRIBUTION

Corresponding radial stress distribution measurements in the front and middle lugs in the AA, AC, AF, BA, and BC directions were made. Near the lug surfaces, hoop stresses predominate over radial stresses. Radial stresses were greater in the front lug compared to the middle lug. Radial stresses generally peaked beneath the surfaces of the front and middle lugs. Figure 7 gives comparative plots of hoop and radial stresses along AB and AC directions in the front lug. Maximum radial stresses were observed near 4 mm in the AC direction.

FINITE ELEMENT MODELLING

To determine residual stresses after overloading, a two-dimensional ABAQUS model of the major cross section of the breech mechanism was constructed. The major cross section is located in the horizontal plane which contains the bore center line. Symmetry about the vertical center plane permits modelling half of the section. The cartesian coordinate system x and y was used. Figure 8 shows the finite element grid in the breech block/ring assembly made up of triangular parabolic elements. Material behavior was modelled as elastic-perfectly plastic with properties commensurate with lower bounds of breech material specifications. An elastic modulus of 30,000 Ksi and a yield stress of 162 Ksi were used in the model.

The first step of the finite element modelling was to overload the breech to 50 percent greater than the normal load of 83 Ksi. During application of this load, highly stressed areas pass the yield point and deform plastically. The second step of the analysis removes the load. The yielded material has taken a permanent set and now has a different shape when unloaded than it had before overloading. The elastic material that surrounds the yielded areas tries to return to its original shape and, in doing so, compresses these areas. This conflict between the relatively large elastic zone and the small localized plastic zones results in favorable compressive residual stresses residing in the former areas of high stress.

In general, plane stress assumption should be used to model thin plates, while plane strain should be used to model thick (infinite) plates. The model was run assuming both plane strain and plane stress using CPE4 and CPS4 elements. The results using plane strain and plane stress were very similar in both magnitude and distribution of residual stresses. To facilitate comparison with experimental cross section residual stress measurements, the plane stress state was the final choice. After the load was applied and removed, residual stresses between nodes were evaluated by interpolation. Figure 9 shows the contour plots of von Mises and the principal stresses in the front and middle lugs. Residual stress concentrations in the front lug were near the bottom of the lug, slightly shifted towards the back. Surface residual stresses fall off along the sides of the lug centered around maximum stress concentration. In the middle lug, stress concentrations were almost 45 degrees towards the back of the lug.

COMPARISON OF EXPERIMENTAL RESULTS AND FEA PREDICTIONS

The comparison between experimental and theoretical residual stress results showed general good agreement in some features and disagreement in other features as described below:

1. Surface residual stress contour. For surface nodes, no shear stresses are expected. Hoop stresses should be the larger of the absolute value of P1 or P2. In Figure 10, experimental and FEA theoretical residual stresses in the front lug are shown as a function of radial angles from normal to the tangent at the bottom of the lug. The FEA results were obtained from nodal residual stress tensor data. Surface nodal locations for each node were converted to angles made with respect to the normal as shown in Figure 4. Very good agreement between experiment and FEA was observed. Considering the fact that surface stress measurements were performed at 0.5 mm depth due to finite collimator size correction, stress at the surface should be more compressive than what is shown in the figure, and the agreement is actually better than what is shown.

2. Sub-surface residual stress distribution. In Figure 11, a semi-quantitative comparison was made between experimental and FEA hoop stresses at sites AB and AC. Because of the size of the mesh, no FEA nodal residual stress tensor data was available. FEA stress levels were visually extracted from the interpolated stress contour plot as shown in Figure 10. Along AB, experimental hoop direction is tangent to the stress contour. Along AC, experimental hoop direction is no longer tangent to the stress contour and the comparison is approximate. Curvature in the FEA stress distribution is a result of the ABAQUS interpolation algorithm. Experimental stress distributions show thicker but less compressive plastic layers compared to FEA predictions.

3. Maximum stress concentrations. In the front lug, experimental results showed maximum compressive stress near the bottom of the lug that decrease when moving up the sides of the lugs in excellent agreement with FEA analysis. In the middle lug, similar behaviors were observed. However, experimental results showed maximum compressive stress near the BC direction, while FEA predicts maximum stress almost 45 degrees from normal.

An extensive quantitative comparison between experimental and theoretical results is difficult at present because of the x-y geometry chosen for FEA, the radial geometry chosen for experimental analysis, and the size of the FEA surface nodes. Nodes along AA, AB, AC, and BA, BB, BC are not co-linear. Furthermore, given radii of the front and middle lugs of 12.3 mm and 6.7 mm, respectively, extracted thickness of an FEA surface element layer is between 2.0 to 3.0 mm. This is large compared to depths of experimental stress distribution. At locations between finite element nodes, residual stress tensor was not available, and residual stresses were obtained from ABAQUS interpolation algorithm.

CONCLUSION

Residual stress management is one of the most important factors in the multi-lug breech system design. Advantageous residual stresses generated by the overload process have been shown to greatly increase the fatigue life of the multi-lug breech system. In this work, experimental residual stress mapping in the front and middle lugs has been compared to predictions from a two-dimensional ABAQUS finite element model. Experimental and FEA residual stress distribution analyses show very good general agreement, with noted differences in the magnitude, thickness, and distribution of the compressive stress layers. Residual stress distribution shows better agreement in the front lug than the middle lug. Deviations between modelling and experimental results can be attributed to the fact that a two-dimensional instead of a three-dimensional model was used and that experimental measurements were performed on a slice and not on the actual breech ring. The fact that experimental compressive residual stresses were smaller than predicted and that the stress layer was thicker than predicted near the bottom of the lugs indicates that when load is applied, more material yields near the bottom of the lug and the plastic layer is much thicker than predicted.

A suggestion for a future model effort is a three-dimensional ABAQUS model where axial stresses may alter hoop and radial stress distribution--a refined and radially distributed mesh with finer elements. Suggested future experimental research and development include measurements in the entire breech ring and real-time measurements of applied and residual stresses on a thicker slice or on the uncut breech ring. Enhanced biaxial and triaxial x-ray stress analysis can further determine the complete stress tensor at any point in the component as long as it is accessible to x-ray radiations (ref 7). The method facilitates future comparisons between FEA and experimental results.

REFERENCES

1. M.J. Glennon, "XM291 Breech Mechanism Design Philosophy," U.S. Army ARDEC Technical Report ARCCB-TR-91009, Benét Laboratories, Watervliet, NY, February 1991.

2. M. Scavullo, Internal Report, U.S. Army ARDEC, Benét Laboratories, Watervliet, NY, 1992.

3. S.L. Lee and M. Scavullo, "Shot Peening and Overload Residual Stresses to Improve Fatigue Life of the Multi-Lug Breech System," Proceedings of the Fourth International Conference on Residual Stresses, 1994, pp. 894-903.

4. J.H. Underwood, "Residual Stress Effects at a Notch Root in A723 Steel to Extend Fatigue Life," U.S. ARDEC Technical Report ARCCB-TR-95008, Benét Laboratories, Watervliet, NY, February 1995.

5. S.L. Lee, M. Doxbeck, and G. Capsimalis, "X-Ray Diffraction Study of Residual Stresses in Metal Matrix Composite-Jacketed Steel Cylinder Subjected to Internal Pressure," in: *Nondestructive Characterization of Materials IV*, Plenum Press, 1990, pp. 419-427.

6. S.L. Lee, P. O'Hara, V. Olmstead, and G. Capsimalis, "Characterization of an Eccentric Swage Autofrettaged Thick-Walled Steel Cylinder," Proceedings of the ASM International Practical Application of Residual Stress Technology, 1991, pp. 123-129.

7. I.C. Noyan and J.B. Cohen, *Residual Stress, Measurement by Diffraction and Interpretation*, Springer-Verlag, 1987.

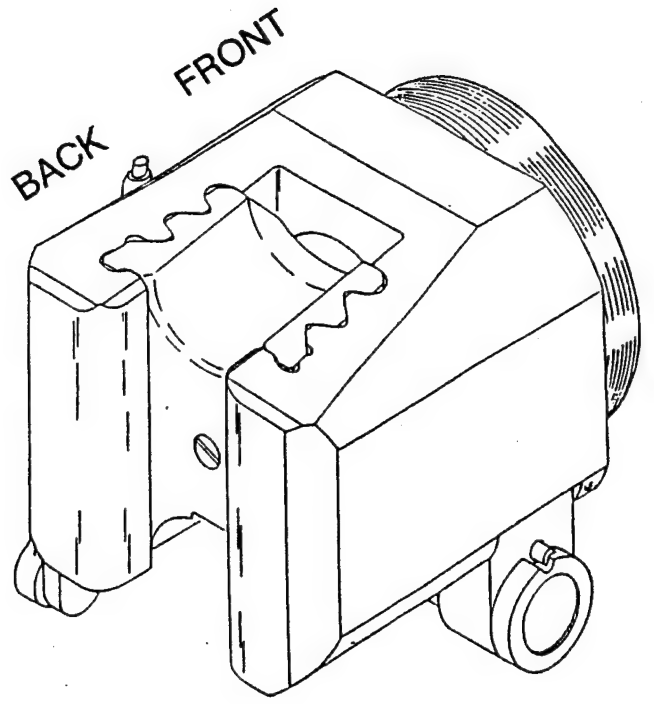

Figure 1 Multi-Lug Breech Block/Ring Assembly, Pressure Load is from the Right

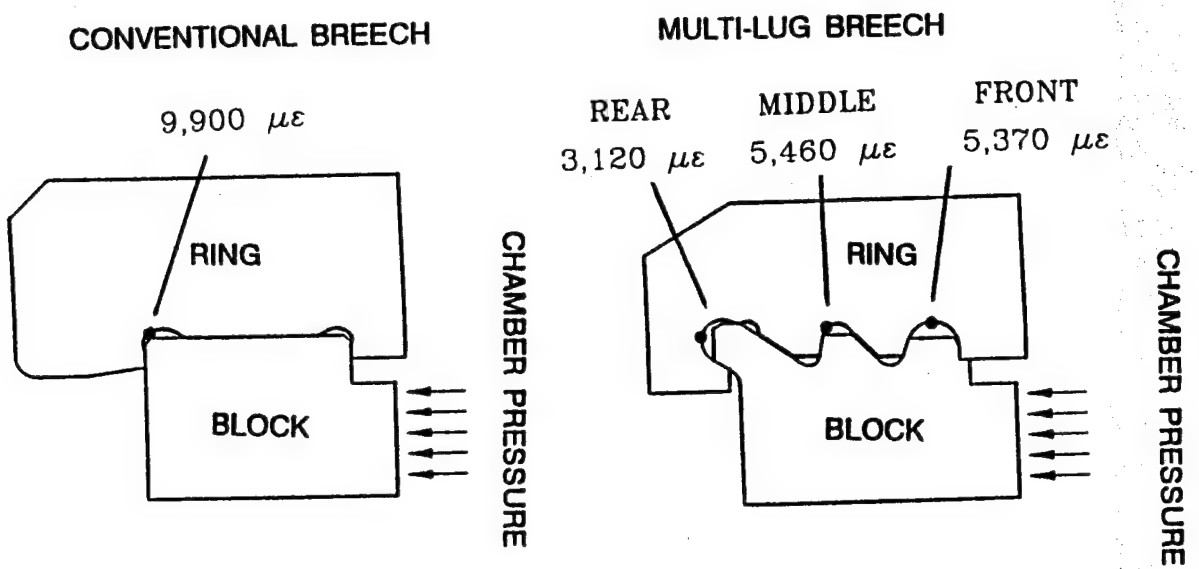

Figure 2 Comparison of Multi-Lug Breech System and Conventional Breech System

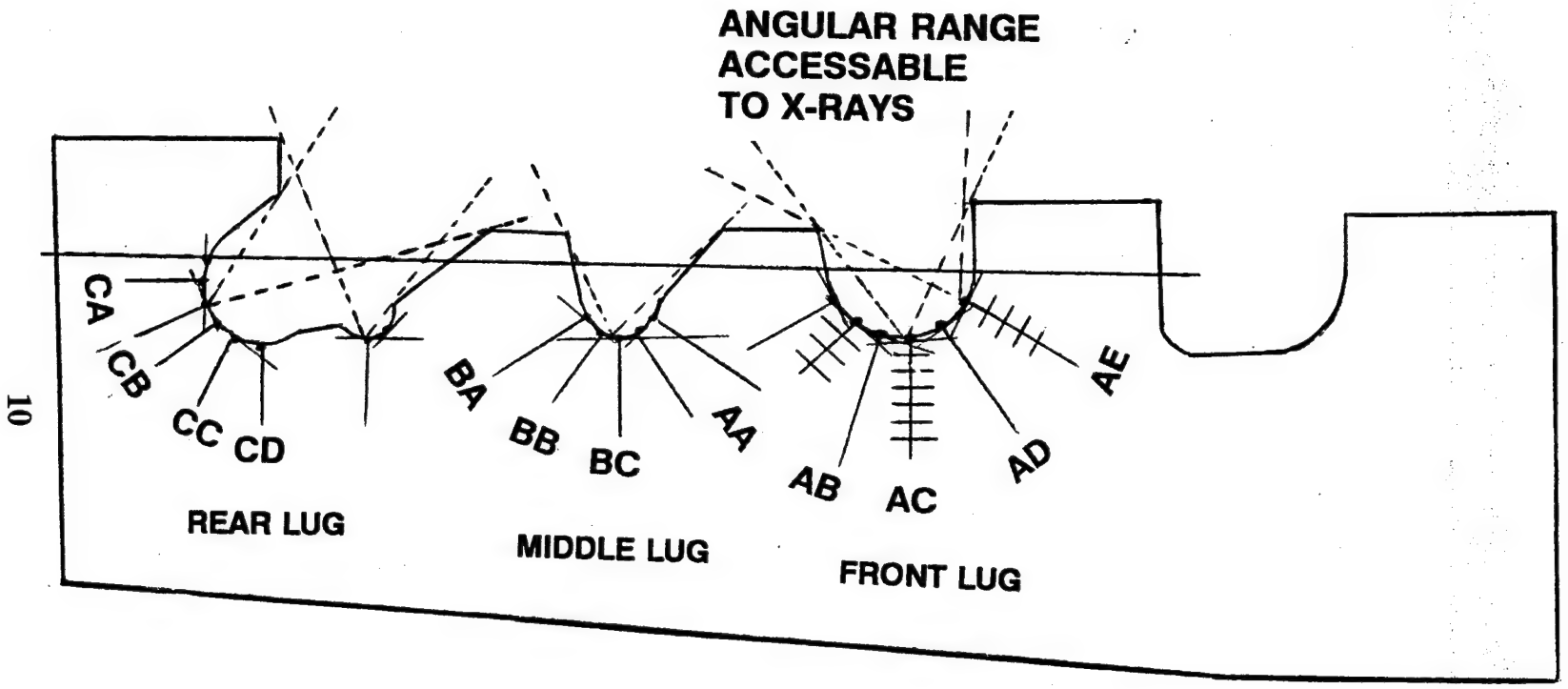

Figure 3 Cross-Sectional and Vertical Residual Stress Analysis in Multi-Lug Breech Ring

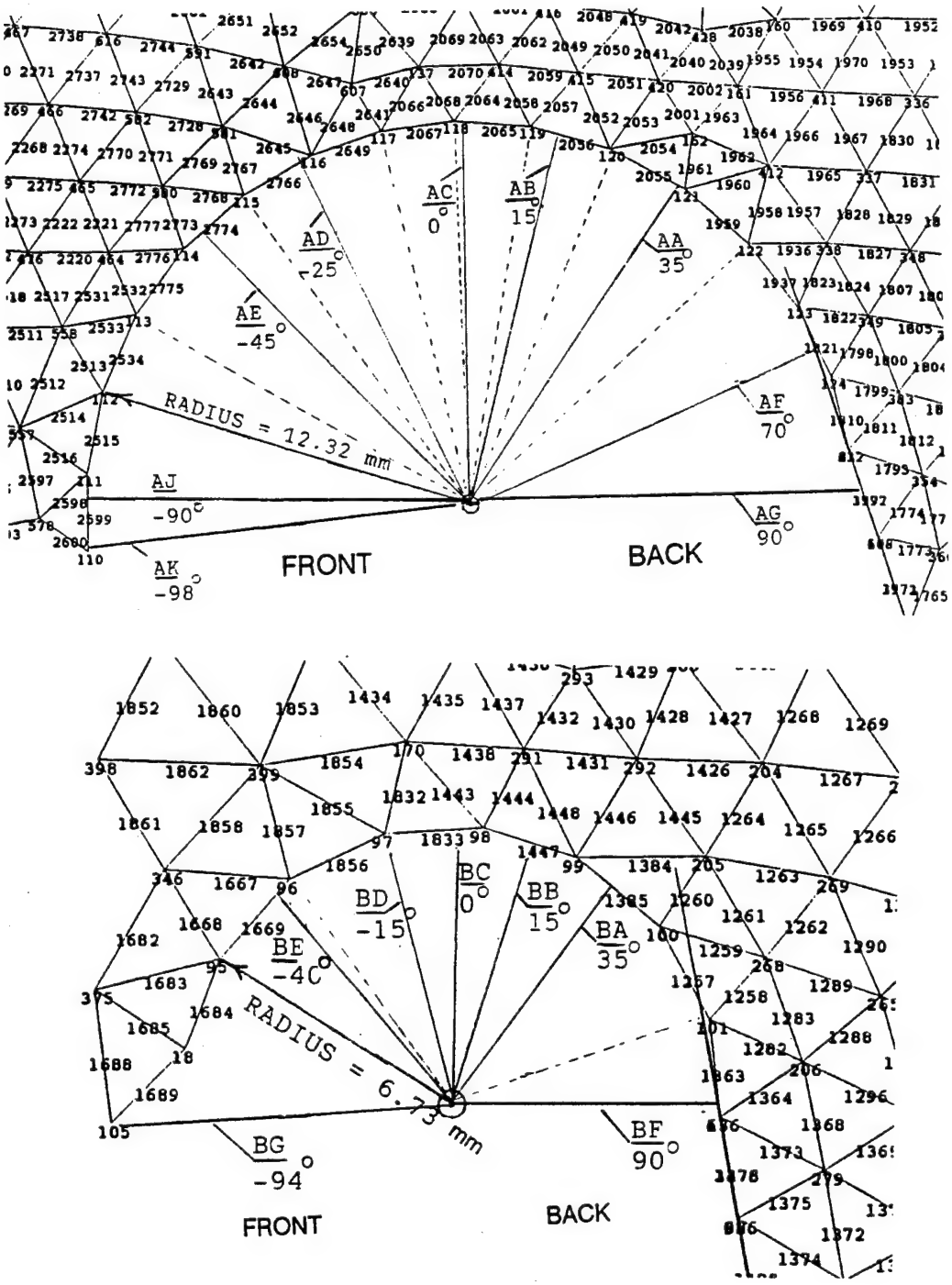

Figure 4 Geometry of Front and Middle Lugs and Directions of X-ray Stress Analysis

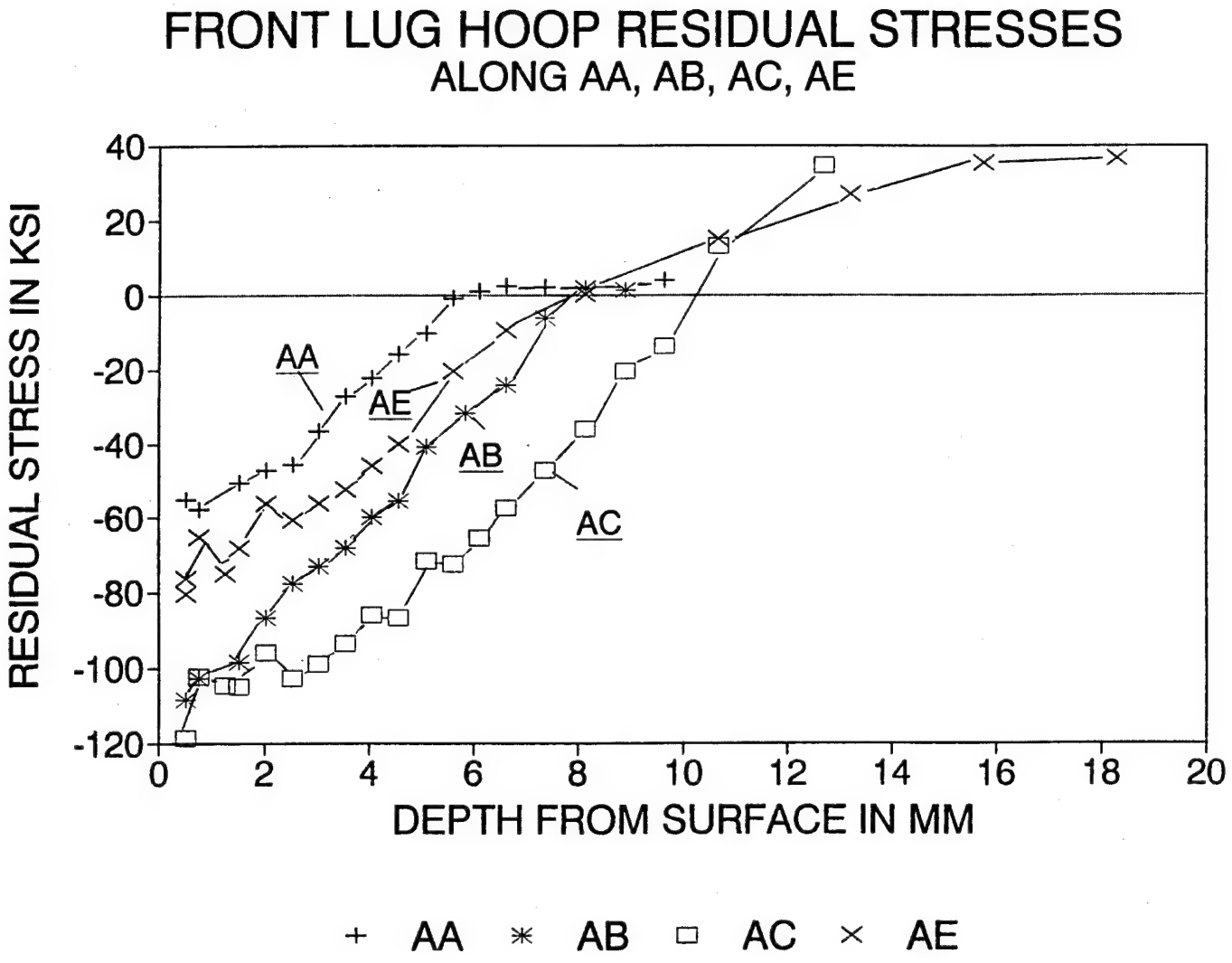

Figure 5 Hoop Residual Stresses in the Front Lug

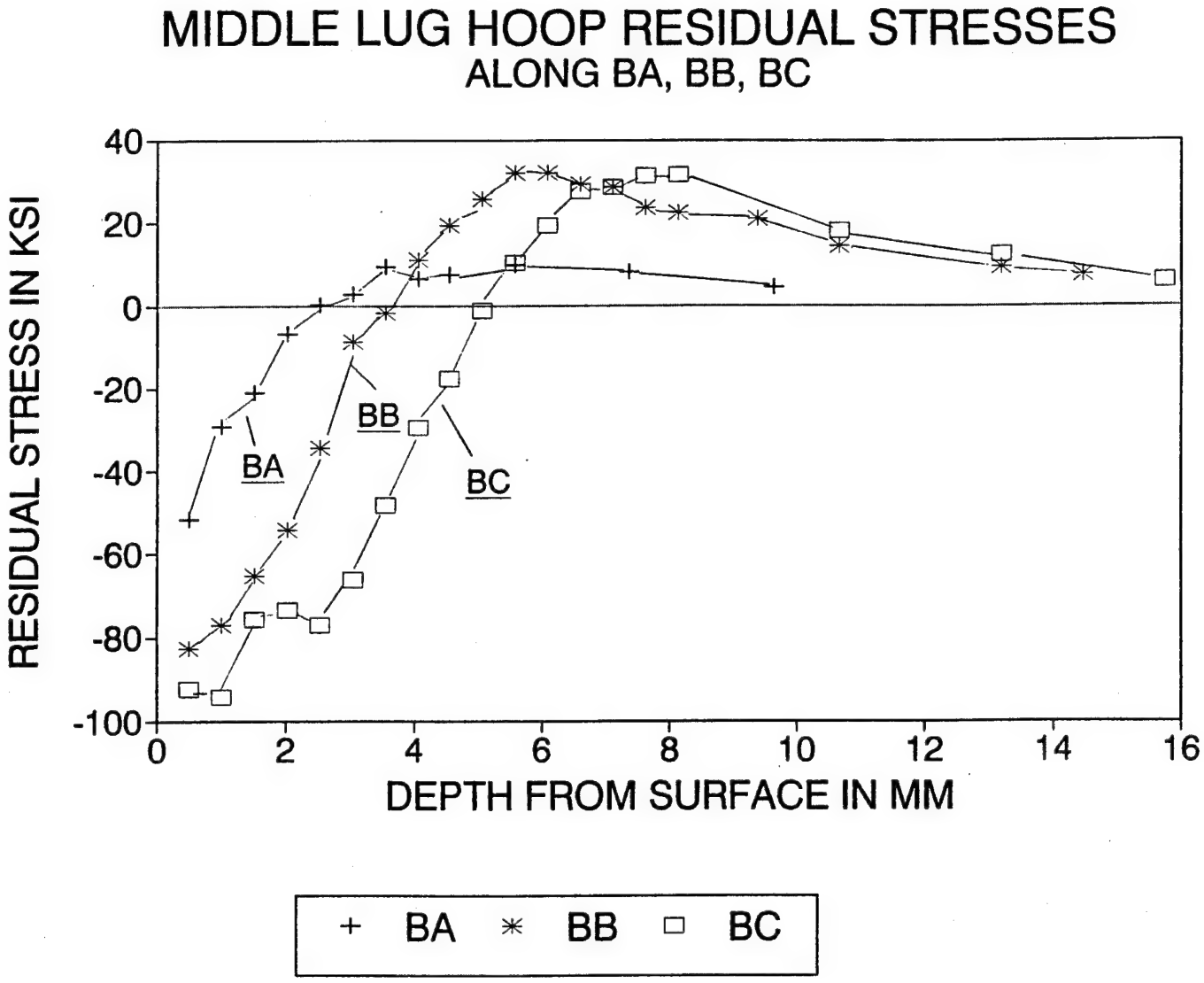

Figure 6 Hoop Residual Stresses in the Middle Lug

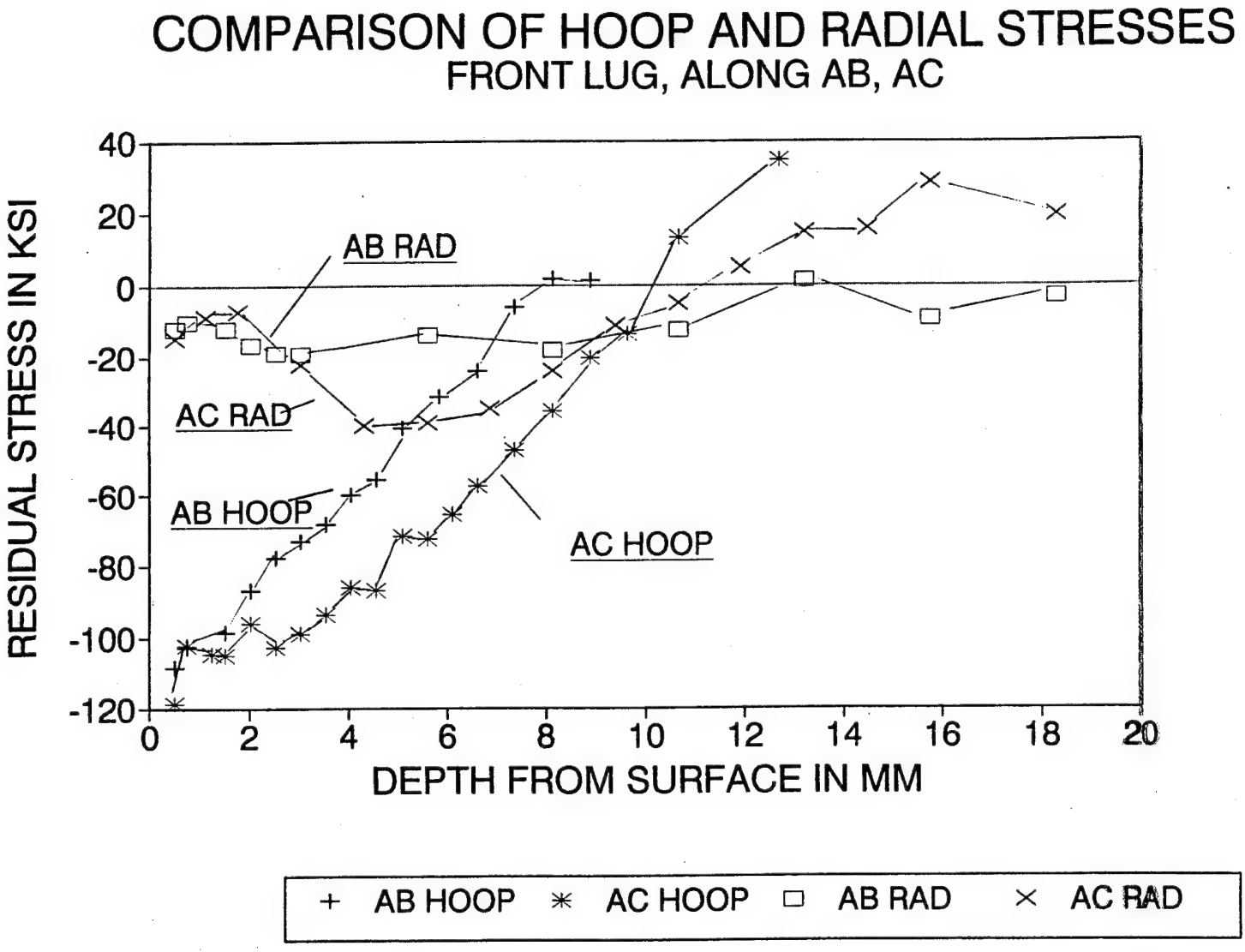

Figure 7 Radial Versus Hoop Residual Stresses in the Front Lug

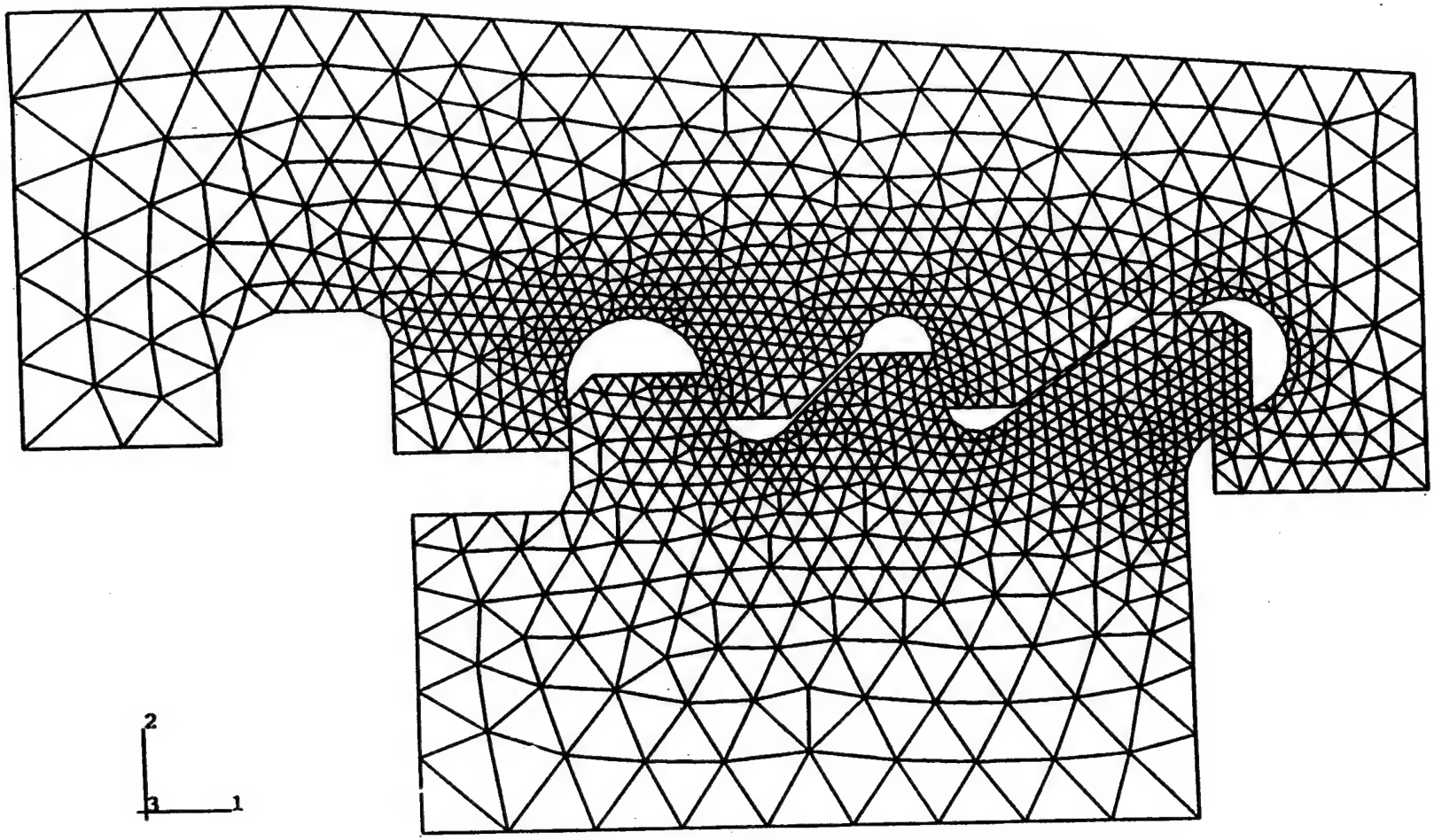

Figure 8 ABAQUS Finite Element Mesh of the Breech Ring/Block Assembly

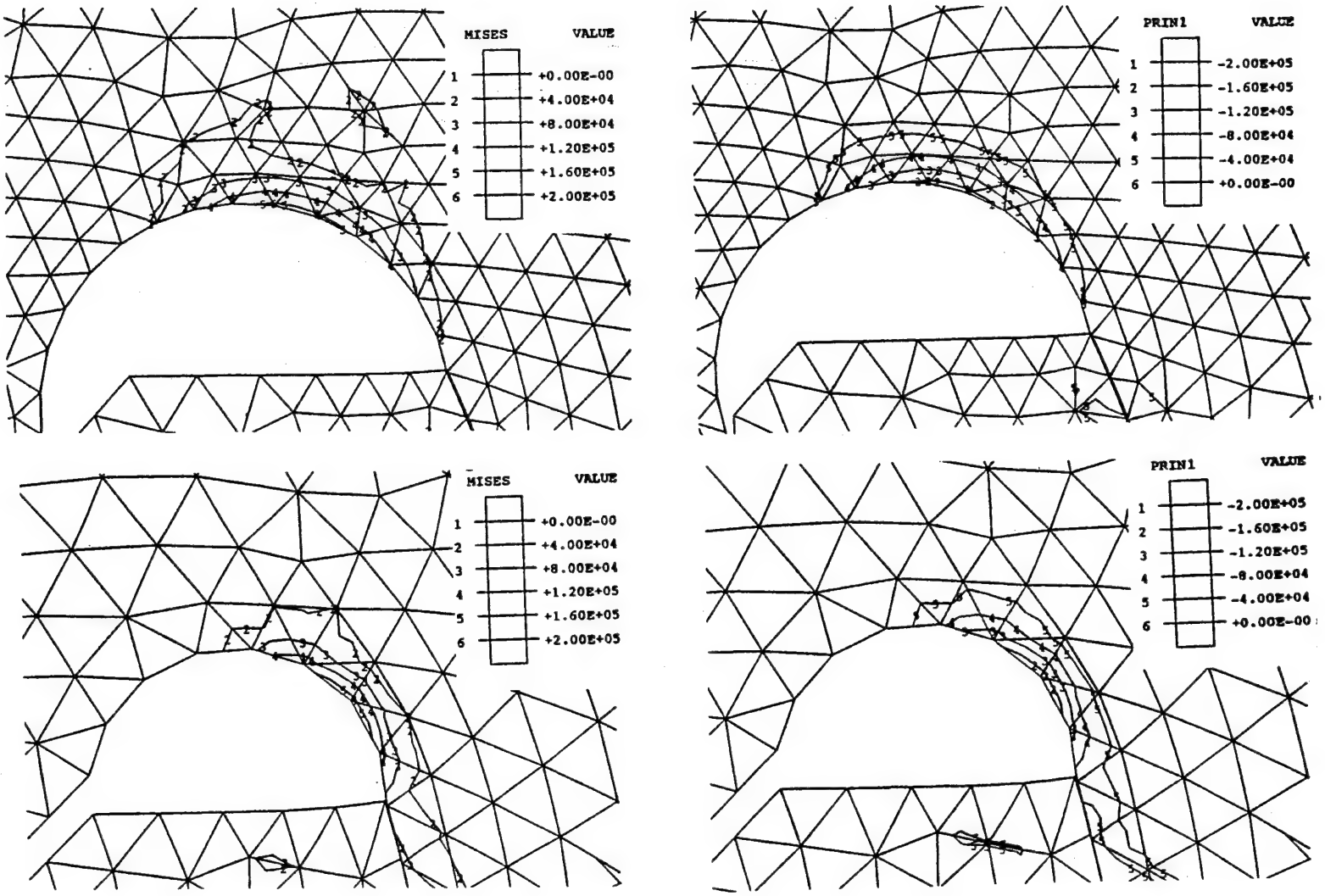

Figure 9 ABAQUS Von Mises and Principal Stresses
top left- front lug mises stresses bottom left- middle lug mises stresses
top right- front lug principal stresses bottom right- middle lug principal stresses

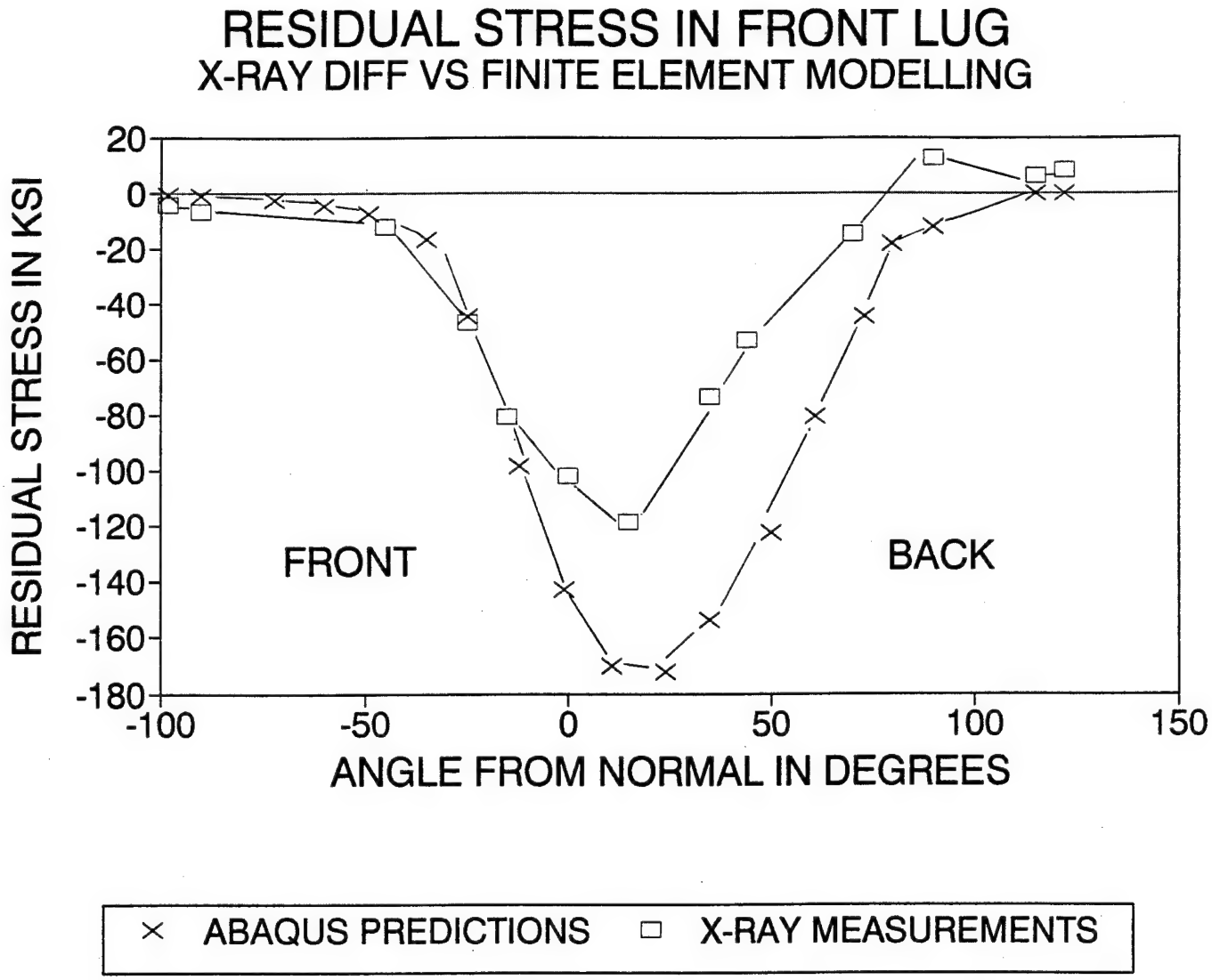

Figure 10 Experimental and ABAQUS Surface Hoop Stress Comparison in the Front Lug

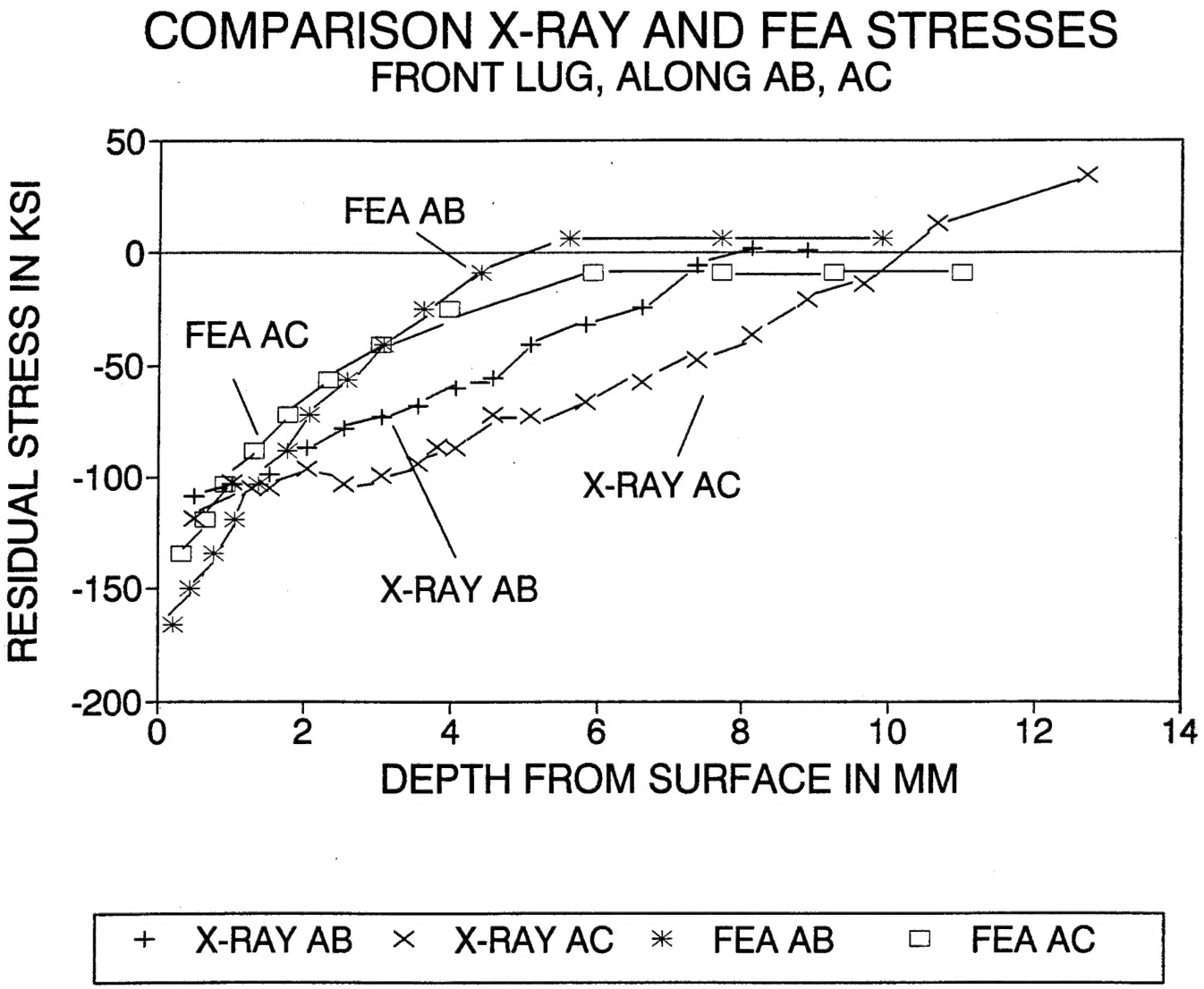

Figure 11 Experimental and ABAQUS Hoop Stress Distribution Comparison in the Front Lug

TECHNICAL REPORT INTERNAL DISTRIBUTION LIST

	NO. OF COPIES
CHIEF, DEVELOPMENT ENGINEERING DIVISION	
ATTN: AMSTA-AR-CCB-DA	1
-DB	1
-DC	1
-DD	1
-DE	1
CHIEF, ENGINEERING DIVISION	
ATTN: AMSTA-AR-CCB-E	1
-EA	1
-EB	1
-EC	
CHIEF, TECHNOLOGY DIVISION	
ATTN: AMSTA-AR-CCB-T	2
-TA	1
-TB	1
-TC	1
TECHNICAL LIBRARY	
ATTN: AMSTA-AR-CCB-O	5
TECHNICAL PUBLICATIONS & EDITING SECTION	
ATTN: AMSTA-AR-CCB-O	3
OPERATIONS DIRECTORATE	
ATTN: SMCWV-ODP-P	1
DIRECTOR, PROCUREMENT & CONTRACTING DIRECTORATE	
ATTN: SMCWV-PP	1
DIRECTOR, PRODUCT ASSURANCE & TEST DIRECTORATE	
ATTN: SMCWV-QA	1

NOTE: PLEASE NOTIFY DIRECTOR, BENÉT LABORATORIES, ATTN: AMSTA-AR-CCB-O OF ADDRESS CHANGES.

TECHNICAL REPORT EXTERNAL DISTRIBUTION LIST

	NO. OF COPIES
ASST SEC OF THE ARMY RESEARCH AND DEVELOPMENT ATTN: DEPT FOR SCI AND TECH THE PENTAGON WASHINGTON, D.C. 20310-0103	1
ADMINISTRATOR DEFENSE TECHNICAL INFO CENTER ATTN: DTIC-OCP (ACQUISITION GROUP) BLDG. 5, CAMERON STATION ALEXANDRIA, VA 22304-6145	2
COMMANDER U.S. ARMY ARDEC ATTN: SMCAR-AEE	1
SMCAR-AES, BLDG. 321	1
SMCAR-AET-O, BLDG. 351N	1
SMCAR-FSA	1
SMCAR-FSM-E	1
SMCAR-FSS-D, BLDG. 94	1
SMCAR-IMI-I, (STINFO) BLDG. 59 PICATINNY ARSENAL, NJ 07806-5000	2
DIRECTOR U.S. ARMY RESEARCH LABORATORY ATTN: AMSRL-DD-T, BLDG. 305 ABERDEEN PROVING GROUND, MD 21005-5066	1
DIRECTOR U.S. ARMY RESEARCH LABORATORY ATTN: AMSRL-WT-PD (DR. B. BURNS) ABERDEEN PROVING GROUND, MD 21005-5066	1
DIRECTOR U.S. MATERIEL SYSTEMS ANALYSIS ACTV ATTN: AMXSY-MP ABERDEEN PROVING GROUND, MD 21005-5071	1
COMMANDER ROCK ISLAND ARSENAL ATTN: SMCRI-ENM ROCK ISLAND, IL 61299-5000	1
MIAC/CINDAS PURDUE UNIVERSITY P.O. BOX 2634 WEST LAFAYETTE, IN 47906	1
COMMANDER U.S. ARMY TANK-AUTMV R&D COMMAND ATTN: AMSTA-DDL (TECH LIBRARY) WARREN, MI 48397-5000	1
COMMANDER U.S. MILITARY ACADEMY ATTN: DEPARTMENT OF MECHANICS WEST POINT, NY 10966-1792	1
U.S. ARMY MISSILE COMMAND REDSTONE SCIENTIFIC INFO CENTER ATTN: DOCUMENTS SECTION, BLDG. 4484 REDSTONE ARSENAL, AL 35898-5241	2
COMMANDER U.S. ARMY FOREIGN SCI & TECH CENTER ATTN: DRXST-SD 220 7TH STREET, N.E. CHARLOTTESVILLE, VA 22901	1
COMMANDER U.S. ARMY LABCOM MATERIALS TECHNOLOGY LABORATORY ATTN: SLCMT-IML (TECH LIBRARY) WATERTOWN, MA 02172-0001	2
COMMANDER U.S. ARMY LABCOM, ISA ATTN: SLCIS-IM-TL 2800 POWER MILL ROAD ADELPHI, MD 20783-1145	1

NOTE: PLEASE NOTIFY COMMANDER, ARMAMENT RESEARCH, DEVELOPMENT, AND ENGINEERING CENTER, BENÉT LABORATORIES, CCAC, U.S. ARMY TANK-AUTOMOTIVE AND ARMAMENTS COMMAND, AMSTA-AR-CCB-O, WATERVLIET, NY 12189-4050 OF ADDRESS CHANGES.

TECHNICAL REPORT EXTERNAL DISTRIBUTION LIST (CONT'D)

	NO. OF COPIES
COMMANDER U.S. ARMY RESEARCH OFFICE ATTN: CHIEF, IPO P.O. BOX 12211 RESEARCH TRIANGLE PARK, NC 27709-2211	1
DIRECTOR U.S. NAVAL RESEARCH LABORATORY ATTN: MATERIALS SCI & TECH DIV CODE 26-27 (DOC LIBRARY) WASHINGTON, D.C. 20375	1 1
WRIGHT LABORATORY ARMAMENT DIRECTORATE ATTN: WL/MNM EGLIN AFB, FL 32542-6810	1
WRIGHT LABORATORY ARMAMENT DIRECTORATE ATTN: WL/MNMF EGLIN AFB, FL 32542-6810	1

NOTE: PLEASE NOTIFY COMMANDER, ARMAMENT RESEARCH, DEVELOPMENT, AND ENGINEERING CENTER, BENÉT LABORATORIES, CCAC, U.S. ARMY TANK-AUTOMOTIVE AND ARMAMENTS COMMAND, AMSTA-AR-CCB-O, WATERVLIET, NY 12189-4050 OF ADDRESS CHANGES.